

# ”Bound luminosity” state in the extended Dicke model

S. S. Seidov<sup>1</sup> and S. I. Mukhin<sup>1</sup>

<sup>1</sup>*Theoretical Physics and Quantum Technologies Department, NUST ”MISIS”, Moscow, Russia*

The extended Dicke model describes interaction of the single-mode electromagnetic resonator with an ensemble of two-level systems. In this paper we obtain quasiclassical equations of motion of the extended Dicke model. For certain initial conditions and range of parameters the equations of motion can be solved analytically via Jacobi elliptic functions. The solution is a ”bound luminosity” state, which was described by the authors previously in [1] for ordinary Dicke model and now is generalized for the case of the extended Dicke model. In this state the periodic beatings of the electromagnetic field in the cavity and the ensemble of two-level systems occur. At the initial moment the energy is stored in the electromagnetic field in the cavity, which is then absorbed by the ensemble of two-level systems and released to the cavity again. Also the chaotic properties of the semiclassical model are investigated numerically.

## I. INTRODUCTION

In this paper we study the quasiclassical dynamics of the extended Dicke model. The extended Dicke model describes interaction of the single-mode electromagnetic resonator with an ensemble of two-level systems [2–4]. At a certain critical value of the coupling between the resonator and the ensemble a superradiant or subradiant (depending on the type of direct interaction between two level systems) phase transition occurs [5–10]. The transition leads to appearance of the macroscopic photonic condensate in the resonator and a consequent change of the quantum mechanical state of the two-level system ensemble.

Previously we have described a ”bound luminosity” state, appearing in quasiclassical dynamics of ordinary Dicke model, i.e. the one with ferromagnetic direct interaction between two-level systems in the ensemble [1]. In this state the periodic process of energy transfer between two-level systems and the electromagnetic field in the cavity occurs. Suppose that at some initial moment the ensemble is in its ground state and all energy of the system is stored in the photonic condensate in the cavity. Then the energy of the photonic condensate will transfer to the ensemble, leading to decay of electromagnetic field in the cavity and in transition of two-level systems in their excited state. After that the energy will be again transferred to the condensate and the process will repeat. In this paper we obtain analytical expressions,

describing this beatings.

The paper is structured as follows. First we consider the extended Dicke model Hamiltonian and obtain quasiclassical equations of motion of corresponding quantum observables. Obtained equations of motions are solved in a certain approximation and solutions, describing "bound luminosity" state, are found analytically. These solutions generalize our previous result, obtained for particular case of ordinary (i.e. not extended) Dicke model [1].

## II. DYNAMICS OF THE EXTENDED DICKE MODEL

The extended Dicke model is describing the interaction of  $N$  two-level systems with a single mode electromagnetic resonator. Each two level system is described as a spin-1/2 by Pauli matrices  $\hat{\sigma}_i^{x,y,z}$ , and the electromagnetic wave in the resonator is described as an oscillator with coordinate  $\hat{q}$  and momentum  $\hat{p}$ . The Hamiltonian is

$$\hat{H} = \frac{\hat{p}^2 + \omega^2 \hat{q}^2}{2} + g\hat{p}\hat{S}_y - \omega_0\hat{S}_z + (1 + \varepsilon)\frac{g^2}{2}\hat{S}_y^2, \quad (1)$$

where  $\omega$  is the resonator frequency,  $g$  is the coupling constant,  $\omega_0$  is the energy distance between energy levels of two-level systems,  $\varepsilon$  describes direct inter-spin interaction and total spin projections

$$\hat{S}_{x,y,z} = \sum_{i=1}^N \hat{\sigma}_i^{x,y,z} \quad (2)$$

were introduced.

### A. Quasiclassical equations of motion

First we obtain the Heisenberg equations of motion for operators  $\hat{p}$ ,  $\hat{q}$ ,  $\hat{S}_{x,y,z}$  via their commutator with the Hamiltonian:

$$\dot{\hat{A}} = i[\hat{H}, \hat{A}], \quad \hat{A} = \hat{p}, \hat{q}, \hat{S}_{x,y,z}. \quad (3)$$

Following expressions arise due to  $\hat{S}_y^2$  term in the Hamiltonian:

$$\begin{aligned} [\hat{S}_z, \hat{S}_y^2] &= i\hat{S}_x\hat{S}_y + i\hat{S}_y\hat{S}_x \\ [\hat{S}_x, \hat{S}_y^2] &= i\hat{S}_y\hat{S}_z + i\hat{S}_z\hat{S}_y. \end{aligned} \quad (4)$$

In quasiclassical approximation we replace the quantum-mechanical operators with real valued functions which commute with each other, thus the r.h.s in (4) just turns into  $2S_xS_y$  and  $2S_zS_y$ . This can be justified by noticing, that the commutator of two operators  $[\hat{S}_i, \hat{S}_j] \sim \hbar$  and  $\hbar \rightarrow 0$

in the quasiclassical limit. Finally, the quasiclassical equations of motion are

$$\begin{aligned}
\dot{S}_z &= -gpS_x - (1 + \varepsilon)g^2S_xS_y \\
\dot{S}_x &= gpS_z + \omega_0S_y + (1 + \varepsilon)g^2S_yS_z \\
\dot{S}_y &= -\omega_0S_x \\
\dot{p} &= -\omega^2q \\
\dot{q} &= p + gS_y.
\end{aligned} \tag{5}$$

### B. Stationary points

The phase space of the system is a product  $\mathbb{S}^2 \times \mathbb{R}^2$ , where  $\mathbb{S}^2$  is a sphere — phase space of the spin, and  $\mathbb{R}^2$  is the  $p$ - $q$  plane — phase space of the oscillator. We introduce a vector in the phase-space

$$\mathbf{x} = \left( S_x, S_y, S_z, p, q \right)^T. \tag{6}$$

The stationary points are the points in phase space where the derivatives of  $p$ ,  $q$ ,  $S_{x,y,z}$  vanish. Thus to find them one needs to solve system (5) with left hand side equal to zero. The resulting stationary points are

$$\begin{aligned}
\mathbf{x}_\pm^{\text{pole}} &= \left( 0, 0, \pm S, 0, 0 \right)^T \\
\mathbf{x}_\pm &= \left( 0, \pm \sqrt{S^2 - \frac{\omega_0^2}{\varepsilon^2 g^4}}, -\frac{\omega_0}{\varepsilon g^2}, \mp g \sqrt{S^2 - \frac{\omega_0^2}{\varepsilon^2 g^4}}, 0 \right)^T.
\end{aligned} \tag{7}$$

The first two stationary points  $\mathbf{x}_\pm^{\text{pole}}$  correspond to spin aligned along  $z$ -axis and the oscillator being at the origin of the  $p$ - $q$  plane. Other two stationary points  $\mathbf{x}_\pm$  exist when

$$S^2 - \frac{\omega_0^2}{\varepsilon^2 g^4} > 0 \Rightarrow g > g_c = \sqrt{\frac{\omega_0}{|\varepsilon|S}}. \tag{8}$$

For  $\varepsilon \leq 1$  these points correspond to superradiant phase in which the spin alignes itself along the  $y$  axis and non-zero average of photonic momentum  $p$  appears. The  $y$  component of the spin at  $\mathbf{x}_\pm$  can be written as

$$S_y \Big|_{\mathbf{x}_\pm} = \pm S \sqrt{1 - \frac{g_c^4}{g^4}}. \tag{9}$$

Together with the expression (8) for the critical coupling constant and given that  $p \Big|_{\mathbf{x}_\pm} = -gS_y \Big|_{\mathbf{x}_\pm}$  this reproduces known results for the superradiant phase transition [5, 8]. Also it was shown previously that for  $\varepsilon = 0$  the critical coupling constant tends to infinity [9, 10], which is also in agreement with (8).

### 1. Stability of fixed points

The Hamiltonian, as a function of canonical variables, has extrema at the fixed points of the corresponding system of equations of motion. The stability of the fixed point is then determined by the type of the extremum i.e. by it being a maximum or a minimum. Thus, first we should express the spin variables in the Hamiltonian (1) through canonical variables. We choose them as  $S_z$  and  $\varphi$ , where  $\varphi$  is the angle of rotation around  $z$ -axis and  $\{\varphi, S_z\} = 1$ . Then the Hamiltonian is

$$H = \frac{p^2 + \omega^2 q^2}{2} + gp\sqrt{S^2 - S_z^2} \sin \varphi - \omega_0 S_z + (1 + \varepsilon) \frac{g^2}{2} (S^2 - S_z^2) \sin^2 \varphi. \quad (10)$$

One of the fixed points, obtained from conditions  $\partial_q H = 0$ ,  $\partial_p H = 0$  and  $\partial_\varphi H = 0$  are  $q = 0$ ,  $p = \pm g\sqrt{S^2 - S_z^2}$ ,  $\varphi = \mp\pi/2$ . These are the fixed points  $\mathbf{x}_\pm$ , but expressed via variables  $S_z$  and  $\varphi$ . Next we substitute this values to the Hamiltonian in order to study its extrema structure with respect to variable  $S_z$ . The result is

$$h = -\omega_0 S_z + \frac{\varepsilon g^2}{2} (S^2 - S_z^2). \quad (11)$$

It is convenient to introduce angle  $\gamma$  of rotation in  $z$ - $y$  plane such that  $S_z = S \cos \gamma$  and  $S_y = S \sin \gamma$ . Then finally we have to find the extrema of the function

$$U(\gamma) = -\omega_0 S \cos \gamma + \frac{\varepsilon g^2}{2} S^2 \sin^2 \gamma. \quad (12)$$

For  $g < g_c$  the function has extrema at  $\gamma_0 = 0 + 2\pi n$  and  $\gamma_\pi = \pi + 2\pi n$ ,  $n \in \mathbb{Z}$ . These angles correspond to  $S_z = \pm S$ , i.e. the fixed points  $\mathbf{x}_\pm^{\text{pole}}$ . The points  $\gamma_0$  are stable minimums and  $\gamma_\pi$  are unstable maximums for all values of  $\varepsilon$ . The minimums  $\gamma_0$  for which  $S_z = -S$  correspond to the normal phase of the Dicke model, stable for  $g < g_c$ .

For  $g > g_c$  new extrema of  $U$  appear for  $\gamma_{\text{sr}}$  such that  $\cos \gamma_{\text{sr}} = -\omega_0/(\varepsilon g^2 S)$ . These points correspond to points  $\mathbf{x}_\pm$  and describe the superradiant phase. They are local minimums if  $\varepsilon < 0$  and local maximums if  $\varepsilon > 0$ . Thus we conclude, that the superradiant phase is stable for negative  $\varepsilon$  and unstable for positive  $\varepsilon$ . Accordingly, the extrema  $\gamma_0$  and  $\gamma_\pi$  turn into local maximums if  $\varepsilon < 0$  and into local minimums if  $\varepsilon > 0$ . The latter means, that the spin remains aligned along  $z$ -axis even for  $g > g_c$ , manifesting the stability of the subradiant phase for  $\varepsilon > 0$ . Plots of  $U(\gamma)$  are presented in fig. 1.

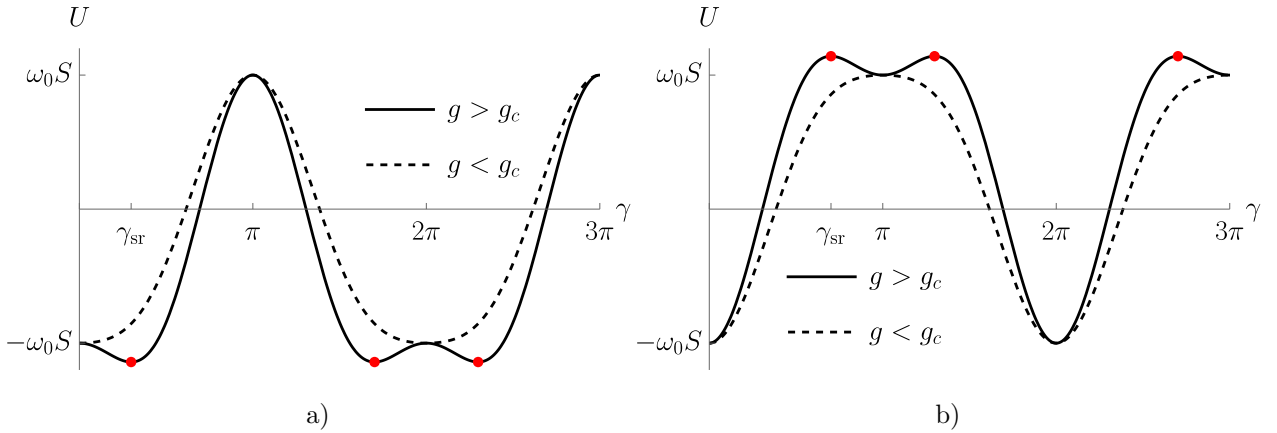


Figure 1. Plots of the function  $U(\gamma)$ , determining the stability of the Hamiltonian extrema and accordingly of the fixed points of the equations of motion (5). For  $\varepsilon < 0$  (a) the extrema of  $U$ , corresponding to the superradiant phase (red dots) are minima at  $g > g_c$ . For  $\varepsilon > 0$  (b) they are maxima. Also the maxima at  $\gamma = \pi n$  for  $g > g_c$  and  $\varepsilon < 0$  turn into minima for  $\varepsilon > 0$ .

### C. Bound luminosity solution for $p \approx -gS_y$

Let us consider the case, when the displacement of the oscillator is small and  $\dot{q} \approx 0, \dot{p} \approx 0$ . Then from last two equations of (5) we obtain

$$\begin{aligned} q &\approx 0 \\ p &\approx -gS_y. \end{aligned} \tag{13}$$

Next we substitute this in the first three equation in (5) and obtain differential equations for spin projections:

$$\begin{aligned} \dot{S}_z &= -\varepsilon g^2 S_x S_y \\ \dot{S}_x &= \omega_0 S_y + \varepsilon g^2 S_y S_z \\ \dot{S}_y &= -\omega_0 S_x. \end{aligned} \tag{14}$$

This system can be solved analytically. First we take the time-derivative of the last equation, express from it  $\dot{S}_x$  and substitute in the second one:

$$\ddot{S}_y = -\omega_0^2 S_y - \omega_0 \varepsilon g^2 S_y S_z. \tag{15}$$

Then we express  $S_x$  from the last equation and substitute in the first one:

$$\dot{S}_z = \frac{\varepsilon g^2}{\omega_0} \dot{S}_y S_y = \frac{\varepsilon g^2}{2\omega_0} \frac{d}{dt} (S_y^2) \Rightarrow S_z = \frac{\varepsilon g^2}{2\omega_0} S_y^2 + C, \tag{16}$$

where  $C$  is the arbitrary constant. Substituting in (15) one obtains an equation for  $S_y(t)$ , which can be solved via Jacobi elliptic functions:

$$\ddot{S}_y = -\omega_0^2 S_y - \frac{\varepsilon^2 g^4}{2} S_y \left( S_y^2 + 2C \frac{\omega_0}{\varepsilon g^2} \right). \tag{17}$$

### 1. Analysis using conservation laws

Before solving the equation, it is instructive to use conservation laws for understanding properties of the resulting trajectories. If one substitutes  $q = 0$  and  $p = -gS_y$  in the Hamiltonian (1), the following expression is obtained:

$$H \Big|_{\substack{q=0 \\ p=-gS_y}} = -\omega_0 S_z + \frac{\varepsilon}{2} g^2 S_y^2 = -\omega_0 C. \quad (18)$$

So there is a corresponding energy conservation law and the second conservation law is the conservation of total spin:  $S_x^2 + S_y^2 + S_z^2 = S^2$ . Thus the trajectory of the system should lay on the intersection of two surfaces defined by conservation laws, this is shown in fig. 2. Similar results were obtained in [11], when considering the LMG–model, which has the Hamiltonian with structure like equation (18).

Depending on the energy the intersection of two surfaces forms a continuous curve separates in to two distinct curves. In the superradiant regime at  $g > g_c$  when the normal phase is unstable, continuous trajectories correspond to meandering of the system between two stable superradiant phases, and separated trajectories — to oscillations around a single stable point.

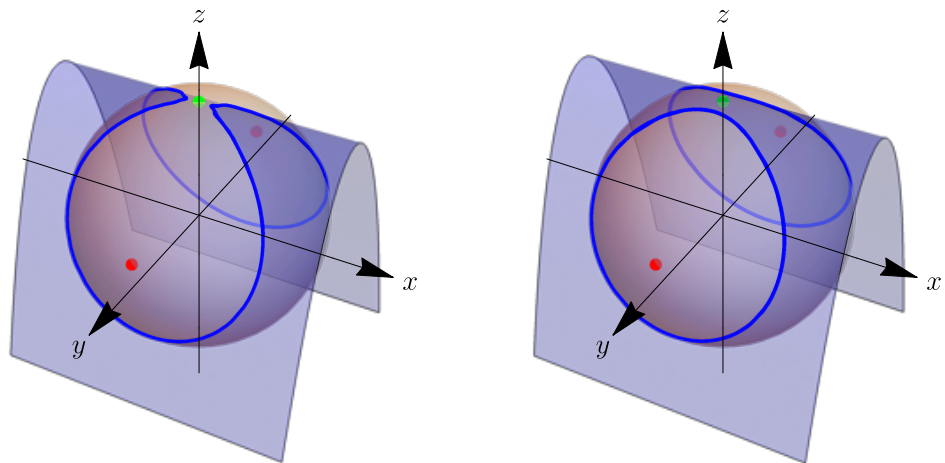


Figure 2. A single curve and two separate curves type phase portraits of system (14) on the total spin sphere  $S_x^2 + S_y^2 + S_z^2 = S^2$ . Blue surface is the surface of constant energy defined by Hamiltonian (18). Red dots — stationary points  $\mathbf{x}_\pm$ , green dot — stationary point  $\mathbf{x}_+^{\text{pole}}$ . The plots are made for  $\varepsilon < 0$ . For  $\varepsilon > 0$  the plot constant energy surface is mirrored with respect to  $x$ – $y$  plane.

## 2. Solution of the equation of motion

In this section we return to equation (17). We rewrite it as

$$\frac{\ddot{S}_y}{\omega_0 S} = -\frac{\omega_0}{2} \left[ \frac{g}{g_c} \right]^4 \left( \frac{S_y}{S} \right)^3 - \omega_0 \left( 1 + \left[ \frac{g}{g_c} \right]^2 \frac{C}{S} \right) \left( \frac{S_y}{S} \right). \quad (19)$$

This is the equation of motion of the particle with the mass  $\omega_0^{-1}$  and coordinate  $x = S_y/S$  in a quartic potential

$$U(x) = \frac{\omega_0}{8} \left[ \frac{g}{g_c} \right]^4 x^4 + \frac{\omega_0}{2} \left( 1 + \left[ \frac{g}{g_c} \right]^2 \frac{C}{S} \right) x^2. \quad (20)$$

Let us consider the following system of differential equations:

$$\begin{aligned} \dot{\theta} &= \frac{\omega_0 g^2}{g_c^2} x \\ \dot{x} &= -\Lambda \sin \theta. \end{aligned} \quad (21)$$

Here  $\Lambda$  is a free parameter, which will be found later. This system has an integral of motion

$$E = \frac{g_c^2}{2\omega_0 g^2} \dot{\theta}^2 - \Lambda \cos \theta. \quad (22)$$

which is the total energy of the system. Now we differentiate the second equation in (21) with respect to time and express the appearing cosine term via energy  $E$ :

$$\ddot{x} = -\Lambda \dot{\theta} \cos \theta = \frac{\omega_0 g^2}{g_c^2} x \left( E - \frac{\omega_0 g^2}{2g_c^2} x^2 \right). \quad (23)$$

This is exactly equation (19) with

$$E = -\frac{\omega_0 g_c^2}{g^2 S} \left( S + \frac{g^2}{g_c^2} C \right). \quad (24)$$

Thus the solution of the equation (19) and consequently the overall dynamical system (14) can be found by finding  $\theta(t)$  from (21). Equation (22) was obtained by us previously when considering dynamics of the non-extended Dicke model, i.e. with  $\varepsilon = -1$  [1].

In order to find  $\theta(t)$  it is convenient to use the conservation law (22). By separating the variables and integrating we obtain

$$\begin{aligned} t &= \frac{g_c}{g} \frac{1}{\sqrt{2\omega_0 \Lambda}} \int_{\theta_0}^{\theta} \frac{d\theta'}{\sqrt{E/\Lambda - \cos \theta'}} = \frac{g_c}{g} \sqrt{\frac{k}{\omega_0 \Lambda}} \left\{ F\left(\frac{\theta}{2}, k\right) - c_0 \right\} \\ k &= \frac{2}{1 + E/\Lambda}. \end{aligned} \quad (25)$$

Here  $\theta_0 = \theta(0)$  and  $c_0$  is the according constant,  $F(u, k)$  is the incomplete elliptic integral of the first kind. The inverse function to the incomplete elliptic integral of the first kind is the Jacobi amplitude  $\text{am}(x, k)$ . Solving for  $\theta$  we obtain

$$\theta = 2 \text{am} \left( \frac{g}{g_c} \sqrt{\frac{\Lambda \omega_0}{k}} t + c_0, k \right). \quad (26)$$

Now for  $S_x$ ,  $S_y$  and  $S_z$  we obtain

$$\begin{aligned} S_y &= \frac{Sg_c^2}{\omega_0 g^2} \dot{\theta} = 2S \frac{g}{g_c} \sqrt{\frac{\Lambda\omega_0}{k}} \operatorname{dn} \left( \frac{g}{g_c} \sqrt{\frac{\Lambda\omega_0}{k}} t + c_0, k \right) \\ S_z &= \frac{g^2}{Sg_c^2} S_y^2 + C \\ S_x &= -\frac{1}{\omega_0} S_y = 2\Lambda S \frac{g^2}{g_c^2} \operatorname{cn} \left( \frac{g}{g_c} \sqrt{\frac{\Lambda\omega_0}{k}} t + c_0, k \right) \operatorname{sn} \left( \frac{g}{g_c} \sqrt{\frac{\Lambda\omega_0}{k}} t + c_0, k \right). \end{aligned} \quad (27)$$

Here  $\operatorname{cn}$ ,  $\operatorname{sn}$  and  $\operatorname{dn}$  are Jacobi elliptic functions. From these equations follows

$$S_x^2 + S_y^2 + S_z^2 = S^2 \left( \frac{\Lambda^2}{\omega_0^2} - \frac{g_c^4}{g_4^2} - \frac{2C}{S} \frac{g_c^2}{g^2} \right). \quad (28)$$

By demanding, that the sum of squares of spin projections equals to square of the total spin we find the value of  $\Lambda$ :

$$S^2 \left( \frac{\Lambda^2}{\omega_0^2} - \frac{g_c^4}{g_4^2} - \frac{2C}{S} \frac{g_c^2}{g^2} \right) = S^2 \Rightarrow \Lambda = \omega_0 \sqrt{1 + \frac{g_c^4}{g^4} + \frac{2C}{S} \frac{g_c^2}{g^2}}. \quad (29)$$

In derivation above we neglected derivatives  $\dot{q}$  and  $\dot{p}$ , see eq. (13), thus introducing error to the solution. Exact solutions with  $\dot{q} = \dot{p} = 0$  are stationary points  $\mathbf{x}_\pm$  in (7). In the approximate solution the photon momentum  $p$  travels between two stationary points  $p_0 = \pm g\sqrt{S^2 - \omega_0^2/(\varepsilon^2 g^4)}$ , see stationary points  $\mathbf{x}_\pm$  in (7). Thus the change of the momentum  $\Delta p \propto 2p_0$  should be small, so that one can neglect the derivative  $\dot{p}$ , which is achieved for  $g \gtrsim g_c$ .

### 3. "Bound luminosity" state

The electric field in the resonator is proportional to the momentum of the oscillator:  $\mathbf{E} \sim p(t) \cos(\omega t)$ , and the dipole moment of the two-level systems in the ensemble is  $\mathbf{d} \sim S_y$ , also the momentum of the photonic oscillator  $p(t) = -gS_y(t)$ . Thus given solutions (27) one obtains the dipole energy of the coupled electromagnetic field and two-level ensemble  $E_{\text{dip}} = \mathbf{E}\mathbf{d} \sim p(t)S_y(t)$  and the Zeeman energy of the spin, associated with the ensemble of two-level systems  $E_Z = -\omega_0 S_z(t)$ . Both energies  $E_{\text{dip}}$  and  $E_Z$  are plotted as functions of time in fig. 3.

From the plot one can clearly see what is the dynamical "bound luminosity" state. Suppose at the initial time the spin is aligned along negative direction of the  $z$ -axis, which minimizes its energy. Then it can absorb the energy of the photonic condensate, which leads to its rotation towards positive direction of the  $z$ -axis. Accordingly, the photonic condensate decays. Next the spin emits back to the resonator, reviving the condensate, rotates into its initial direction and the cycle repeats.

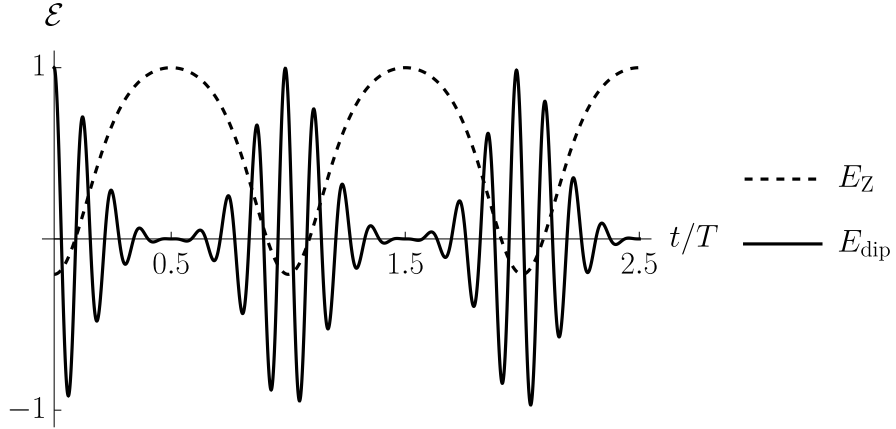


Figure 3. Time dependencies of the Zeeman energy  $E_Z$  of the spin subsystem (dashed line) and the dipole energy  $E_{\text{dip}}$  (solid line) in the bound luminosity state. Both are normalized such that the curves have the same scale on the plot.

#### 4. Connection between motions in a cosine and quartic potential

As it follows from calculations above, there are two perspectives on the considered dynamics. The first one is motion in a potential  $-\Lambda \cos \theta$  with energy  $E$ , eq. (24). And the second one is the motion in a quartic potential (20) with energy

$$\tilde{E} = \frac{\omega_0^2 \dot{x}^2}{2} + U(x) = \frac{\omega_0}{2} \left( 1 - \frac{C}{S} \right). \quad (30)$$

Of course these pictures are connected, as they correspond to the same initial system of equations (14). Let us first determine the allowed values of  $C$  from condition  $E \geq -\Lambda$ , i.e. the motion in the cosine potential can not happen below the bottom of the potential. Thus we obtain

$$\begin{aligned} -S \leq C \leq S, \quad & g \leq g_c \\ -\frac{S}{2} \left( \frac{g_c^2}{g^2} + \frac{g^2}{g_c^2} \right) \leq C \leq S, \quad & g > g_c. \end{aligned} \quad (31)$$

The quartic potential  $U$  has the double-well structure when the coefficient in front of the quadratic term is negative:

$$\frac{\omega_0}{2} \left( 1 + \left[ \frac{g}{g_c} \right]^2 \frac{C}{S} \right) < 0 \Rightarrow C < -S \frac{g_c^2}{g^2}. \quad (32)$$

One can see from (31), that for  $g \leq g_c$  the potential  $U(x)$  always has a single minimum, as values  $C < -Sg_c^2/g^2 < -S$  are forbidden. Accordingly for these values of  $C$  and  $g$  the motion in the cosine potential is happening below the potential barrier, i.e  $E < \Lambda$ .

For  $g > g_c$  the potential  $U(x)$  has a local maximum  $U = 0$  at  $x = 0$  when the condition in (32) is satisfied. Let us start with minimal value of  $C$ , defined in the second line of (31). Then

for motion in the cosine potential  $E > \Lambda$  and for motion in quartic potential  $\tilde{E} = U_{\min}$ , where  $U_{\min}$  is the minimal value of quartic potential  $U(x)$ . As  $C$  grows towards  $C = -S$ , the energy  $E$  of motion in the cosine potential goes up and the energy  $\tilde{E}$  of motion in the quartic potential goes down. Exactly at  $C = -S$  both energies coincide with the maximums of their respective potentials, i.e.  $E = \Lambda$  and  $\tilde{E} = 0$ . And finally when  $C$  achieves its upper bound  $S$ , for motion in cosine potential  $E = -\Lambda$ . This is schematically shown in fig. 4.

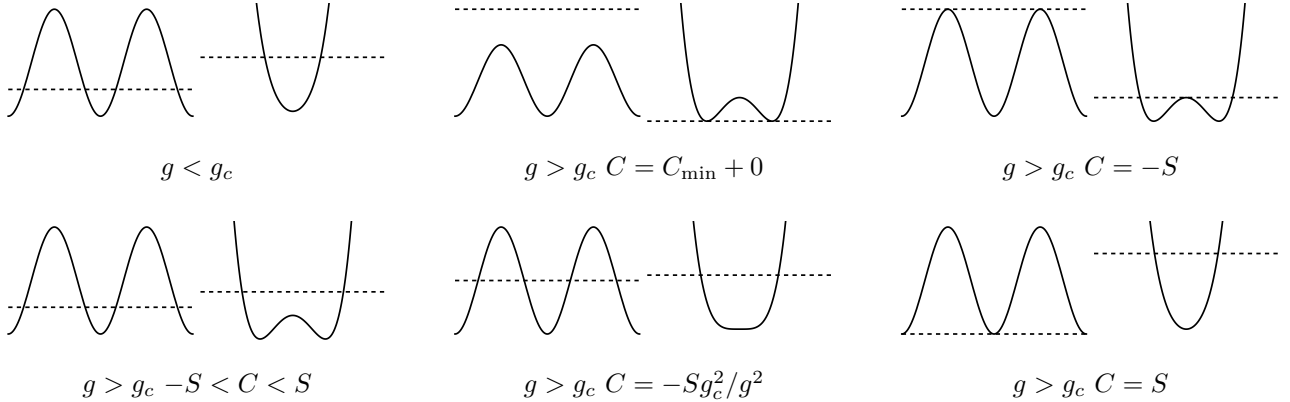


Figure 4. Schematic illustration of correspondence between motions in the cosine and quartic potentials (solid lines). The horizontal dashed lines are values of energy  $E$  of the motion in the cosine potential and  $\tilde{E}$  for motion in a quartic potential.

Energy  $\tilde{E} < 0$ , i.e. below the potential barrier of potential  $U(x)$ , correspond to separated trajectories in section II C 1 and fig. 2 — each around one of the potential minimums. And energies  $\tilde{E} > 0$  above the barrier correspond to continuous trajectories, which travel from one minimum of the potential to another.

#### D. Poincare sections and transition to chaos

It was shown that there is a transition to quantum chaos in the Dicke model at coupling constant  $g = g_c$  [5]. To study this we numerically calculate the Poincare sections of the system (5). Although this is out of the scope of the present paper, Poincare sections of classical systems are strongly related to Wigner and Husimi phase space distributions of its quantum counterpart [12–15]. The Poincare section of a trajectory is constructed by choosing a plane in the phase space of the system and plotting the points at which the trajectory intersects the plane. For a regular (i.e. not chaotic) trajectory the points of the Poincare section lay on a curve. For a chaotic trajectory the section consists of randomly scattered points.

In our case we define the section surface by  $q = 0$  and  $p = p(E)$ , where  $E$  is the total energy of the system. Thus the section is obtained for spin variables  $S_{x,y,z}$ . For convenience of making a

plot we transition to spherical angles  $\theta$  and  $\varphi$ , defined as  $\theta = \arccos(S_z/S)$ ,  $\varphi = \arctan(S_y/S_x)$ . Next we plot Poincare sections on a  $\{\theta, \varphi\}$  plane for trajectories with different initial conditions, see fig. 5. One can see, that at coupling constants well below critical the points are laying on the curves, thus manifesting regular dynamics. As coupling constant grows and approaches critical, more and more chaotic trajectories appear. For couplings above critical the chaotic trajectories fill the entire phase space. This was already shown for ordinary Dicke model ( $\varepsilon = -1$ ) in ref. [5] and we have generalized this result for the extended Dicke model with arbitrary  $\varepsilon$ . An observation from numerical results is made, that for  $\varepsilon > 0$  the transition to chaos is suppressed, meaning that it requires higher energy and ratio  $g/g_c$  to happen.

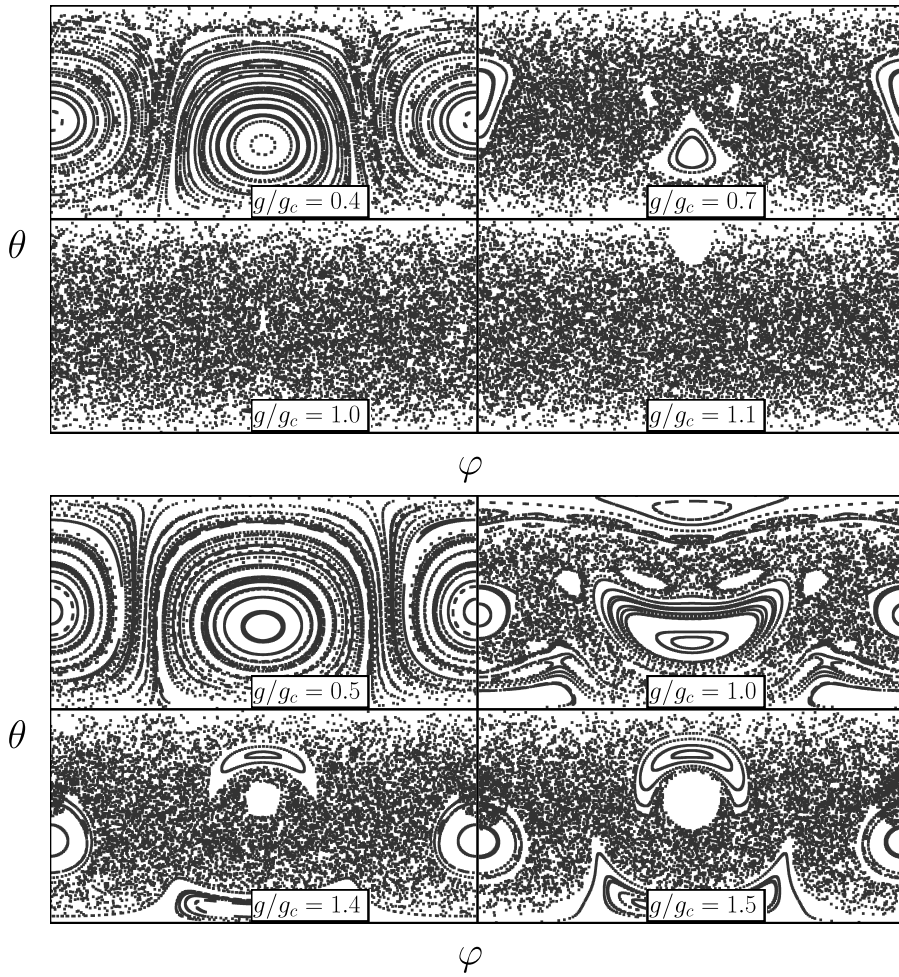


Figure 5. Poincare sections of the system (5). Top plot:  $\varepsilon = -0.5$ ,  $E = 1$ . Down plot:  $\varepsilon = 1$ ,  $E = 2$ . For both plot the rest parameters are chosen as  $\omega = 1$ ,  $\omega_0 = 1$ ,  $S = 1$ . As coupling grows, regular trajectories are destroyed and more chaotic trajectories appear. At couplings higher than critical most of the phase space is chaotic.

### III. CONCLUSIONS

In this work semiclassical equations of motion for extended Dicke model were obtained. In a certain approximation the class of solutions, describing "bound luminosity" state, are expressed analytically using Jacobi elliptic functions. In this state periodic beatings of the electromagnetic field in the cavity and the ensemble of two-level systems occur. Namely, the energy is periodically transferred from the photonic condensate to the ensemble and vice versa. This result generalizes described previously [1] "bound luminosity" state in the ordinary Dicke model to the extended one. The corresponding Hamiltonian, generating this kind of dynamics, appeared to be an LMG-model Hamiltonian. In addition, chaotic properties of the equations of motion were studied numerically by constructing Poincare sections of the system. Also the superradiant and subradiant phase transition phenomena, known to be present in the extended Dicke model, are reproduced by studying the fixed points of the quasiclassical equations of motion.

### IV. ACKNOWLEDGMENTS

This work was supported by the Ministry of Science and Higher Education of the Russian Federation in the framework of the State Program (Project No. 0718-2020-0025) and from the NUST "MISIS" grant No. K2-2022-025 in the framework of the federal academic leadership program Priority 2030.

---

[1] S. Mukhin, A. Mukherjee, and S. Seidov, "Dicke model semiclassical dynamics in superradiant dipolar phase in the "bound luminosity" state," *Journal of Experimental and Theoretical Physics*, vol. 132, p. 658–662, Apr 2021.

[2] R. H. Dicke, "Coherence in spontaneous radiation processes," *Phys. Rev.*, vol. 93, pp. 99–110, Jan 1954.

[3] B. M. Garraway, "The Dicke model in quantum optics: Dicke model revisited," *Philosophical Transactions of the Royal Society A: Mathematical, Physical and Engineering Sciences*, vol. 369, no. 1939, pp. 1137–1155, 2011.

[4] K. Hepp and E. H. Lieb, "On the superradiant phase transition for molecules in a quantized radiation field: the Dicke maser model," *Annals of Physics*, vol. 76, no. 2, pp. 360 – 404, 1973.

[5] C. Emery and T. Brandes, "Chaos and the quantum phase transition in the Dicke model," *Physical review. E, Statistical, nonlinear, and soft matter physics*, vol. 67, p. 066203, 06 2003.

- [6] D. De Bernardis, P. Pilar, T. Jaako, S. De Liberato, and P. Rabl, “Breakdown of gauge invariance in ultrastrong-coupling cavity QED,” *Phys. Rev. A*, vol. 98, p. 053819, Nov 2018.
- [7] T. Jaako, Z.-L. Xiang, J. J. Garcia-Ripoll, and P. Rabl, “Ultrastrong-coupling phenomena beyond the Dicke model,” *Phys. Rev. A*, vol. 94, p. 033850, Sep 2016.
- [8] D. De Bernardis, T. Jaako, and P. Rabl, “Cavity quantum electrodynamics in the nonperturbative regime,” *Phys. Rev. A*, vol. 97, p. 043820, Apr 2018.
- [9] S. I. Mukhin and N. V. Gnezdilov, “First-order dipolar phase transition in the Dicke model with infinitely coordinated frustrating interaction,” *Phys. Rev. A*, vol. 97, p. 053809, May 2018.
- [10] S. S. Seidov and S. I. Mukhin, “Spontaneous symmetry breaking and Husimi Q-functions in extended Dicke model,” *Journal of Physics A: Mathematical and Theoretical*, vol. 53, p. 505301, Nov 2020.
- [11] K. Chinni, P. M. Poggi, and I. H. Deutsch, “Effect of chaos on the simulation of quantum critical phenomena in analog quantum simulators,” *Physical Review Research*, vol. 3, p. 033145, Aug. 2021.
- [12] H. Korsch and W. Leyes, “Quantum and classical phase space evolution: A local measure of delocalization,” *New Journal of Physics*, vol. 4, pp. 1–6215, 08 2002.
- [13] H. J. Korsch and M. V. Berry, “Evolution of Wigner’s phase-space density under a nonintegrable quantum map,” *Physica D: Nonlinear Phenomena*, vol. 3, pp. 627–636, Aug. 1981.
- [14] M. A. Porter, “An Introduction to Quantum Chaos,” 2001.
- [15] L. D’Alessio, Y. Kafri, A. Polkovnikov, and M. Rigol, “From quantum chaos and eigenstate thermalization to statistical mechanics and thermodynamics,” *Advances in Physics*, vol. 65, pp. 239–362, May 2016.